Spin transport parameters in $Ni_{80}Fe_{20}$/Ru and $Ni_{80}Fe_{20}$/Ta bilayers

J. E. Gómez,[1,*] B. Zerai Tedlla,[2] N. R. Álvarez,[1] G. Alejandro,[1] E. Goovaerts,[2] and A. Butera[3]

[1]*Centro Atómico Bariloche, Instituto de Nanociencia y Nanotecnología (CNEA) and Conicet, 8400 Bariloche, Río Negro, Argentina*

[2]*Experimental Condensed Matter Physics, Physics Department, University of Antwerp, Universiteitsplein 1, BE-2610 Antwerpen, Belgium*

[3]*Centro Atómico Bariloche, Instituto de Nanociencia y Nanotecnología (CNEA), Instituto Balseiro (U. N. Cuyo), and Conicet, 8400 Bariloche, Río Negro, Argentina*

(Received 29 May 2014; revised manuscript received 16 October 2014; published 3 November 2014)

We present a systematic study of the spin transport properties in two different bilayer systems, $Ni_{80}Fe_{20}$/Ru and $Ni_{80}Fe_{20}$/Ta, combining ferromagnetic resonance (FMR) and inverse spin Hall effect (ISHE) voltage measurements. We have estimated the effective spin mixing conductance $g^{\uparrow\downarrow}$ by analyzing the permalloy (Py) thickness dependence of the FMR linewidth obtaining $g^{\uparrow\downarrow} = (3.8 \pm 0.7) \times 10^{15}$ cm^{-2} and $g^{\uparrow\downarrow} = (1.3 \pm 0.4) \times 10^{15}$ cm^{-2} for Py/Ru and Py/Ta, respectively. Analyzing the Ta thickness dependence of the ISHE voltage, we have been able to extract the spin diffusion length, $\lambda_{SD} = 1.5 \pm 0.5$ nm, and spin Hall angle, $\Theta_{SH} = -0.03 \pm 0.01$, of Ta. From the two series of Py/Ta bilayers—with thickness variation of ferromagnetic and nonmagnetic layers, respectively—we demonstrate a path to estimate the spin diffusion length from the experimental data, independent of the spin Hall angle and the microwave field amplitude.

DOI: 10.1103/PhysRevB.90.184401 PACS number(s): 81.15.Cd, 76.50.+g, 75.70.Tj, 75.40.Gb

I. INTRODUCTION

The manipulation of the charge and spin degrees of freedom in electron transport has attracted continuous interest in the scientific community for many decades, with a remarkable and persistent revival since the early 1990s [1]. In recent years, the feasibility of spin pumping from a ferromagnetic (FM) layer towards an adjacent nonmagnetic metallic film (NM) was demonstrated in the form of a pure spin current [2,3], which opened paths for the research in several new and novel phenomena in this area [4]. The ability of some metals, like Pt, Pd, or Ta, among others, to convert a spin current into a charge current via the inverse spin Hall effect (ISHE) opens the way to not only qualitative but also quantitative investigation and understanding of the spin transport that takes place in this kind of system.

Earlier studies on inverse spin Hall voltage induced by spin pumping in FM/NM bilayers were carried out using preferably Pt as the NM layer because of its large spin orbit interaction. But several NM metals, like Pd, Mo, Au, and Ta, among others, have been used to demonstrate the spin Hall effect in such metals [5,6]. Applying the theory developed to describe this phenomenon, it is possible to estimate different parameters like the spin diffusion length, the spin Hall angle, or the effective spin mixing conductance. Some of these parameters have a broad range of reported values that depends mainly on the method used for their estimation. For example, spin diffusion length values found for Pt range roughly from 0.5 nm [7] to 10 nm [8]. This broad range can be also explained by spin memory loss effects occurring at the interface [9].

In the following sections we present a detailed study of two different systems of bilayers of permalloy (Py) with Ru and Ta, characterized as a function of the thickness of the FM and/or the NM layer. We show that Ru can effectively be used to detect a spin current by measuring the voltage generated by the inverse spin Hall effect. For both systems we have estimated the effective spin mixing conductance parameter, $g^{\uparrow\downarrow}$. In the case of the Py/Ta bilayer we present a set of spin transport parameters estimated from the Py thickness dependence of the FMR spectra and the inverse spin Hall voltage as a function of the thickness of both the NM and the FM layer. We finally describe a simple method for determining the spin diffusion length independent of the spin Hall angle.

II. FILM FABRICATION AND STRUCTURAL CHARACTERIZATION

Films have been fabricated by dc magnetron sputtering on naturally oxidized Si (100) substrates. The chamber was pumped down to a base pressure of 1×10^{-6} Torr and the films were sputtered at 3 mTorr of Ar pressure, a power of 20 W, and a target-substrate distance of 10 cm. With these parameters we obtained a sputtering rate of 0.06, 0.11, and 0.15 nm/s for Ru, Py, and Ta, respectively. Two different series were grown keeping fixed the NM layer: $t_{Ru} = 10$ nm and $t_{Ta} = 5$ nm and varying the thickness of the Py layer, $t_{Py} = 5$, 7, 9, and 11 nm. Complementarily, another series was grown with different Ta layer thickness, $t_{Ta} = 2$, 5, 8, and 11 nm, and with Py thickness $t_{Py} = 10$ nm (see Table I). Our sputtering machine can host several substrates at the same time, allowing one to deposit a complete series in exactly the same sputtering conditions. In the case of Ta films the sputtering variables were optimized in order to promote the growth of the crystallographic β phase, as confirmed by x-ray diffraction patterns performed on 133 nm reference films, with a high electrical resistivity ($\rho \sim 2000\ \Omega$ nm). Although there is a tendency in very thin Ta films to grow in an amorphous phase, there are several reports in which it is shown that by choosing the correct sputtering conditions the β phase is dominant down to thicknesses of a few nanometers [10–13]. However, possible mixing of both phases should not be totally discarded, especially in the thinnest samples studied in this work ($t_{Ta} = 2$ nm).

FMR spectra were acquired at room temperature with a commercial Bruker ESP 300 spectrometer at frequencies of

*gomezj@cab.cnea.gov.ar

TABLE I. Nominal layer thickness in the three different series of bilayers.

Series 1		Series 2		Series 3	
t_{Py} (nm)	t_{Ru} (nm)	t_{Py} (nm)	t_{Ta} (nm)	t_{Py} (nm)	t_{Ta} (nm)
5	10	5	5	10	2
7	10	7	5	10	5
9	10	9	5	10	8
11	10	11	5	10	11

9.4 GHz (X band), 24 GHz (K band), and 34 GHz (Q band). The samples were placed at the center of a resonant cavity where the derivative of the absorbed power was measured using a standard field modulation and lock-in detection technique, with a modulation frequency of 100 kHz and a modulation amplitude of 10 Oe. The film plane was in all cases parallel to the microwave excitation field. Angular variations with respect to the external dc field were made around a vertical axis parallel to the microwave field (see Fig. 1).

The inverse spin Hall voltage (V_{ISHE}) has been acquired by measuring the voltage between the edges of the sample [see sketch of Fig. 1(a)], while the external magnetic field was swept in the vicinity of the resonance field of the ferromagnet. Electrical contacts were made with two 25 μm diameter aluminum wires fixed to the nonmagnetic layer of the sample with silver paste. The signal was amplified by a high-gain calibrated differential amplifier located close to the cavity to reduce electronic noise. The amplified signal was connected to the digitizer input of the FMR spectrometer in order to synchronize this signal with the magnetic field sweep. The ISHE measurements were all performed inside of the X-band TE102 rectangular cavity (microwave frequency of 9.4 GHz) and with the field modulation turned off.

III. EXPERIMENTAL RESULTS AND DISCUSSION

A. Effective spin mixing conductance in Ru and Ta series

We have measured the FMR spectra and the inverse spin Hall voltage in the whole set of samples. In Fig. 2 we show

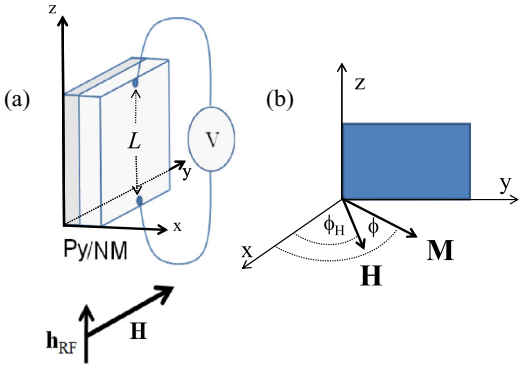

FIG. 1. (Color online) (a) Sketch of the geometrical setup of the sample, the microwave field ($\mathbf{h}_{RF}$), and the external dc field, $\mathbf{H}$. (b) Coordinate reference system chosen to analyze the FMR and the inverse spin Hall voltage measurements.

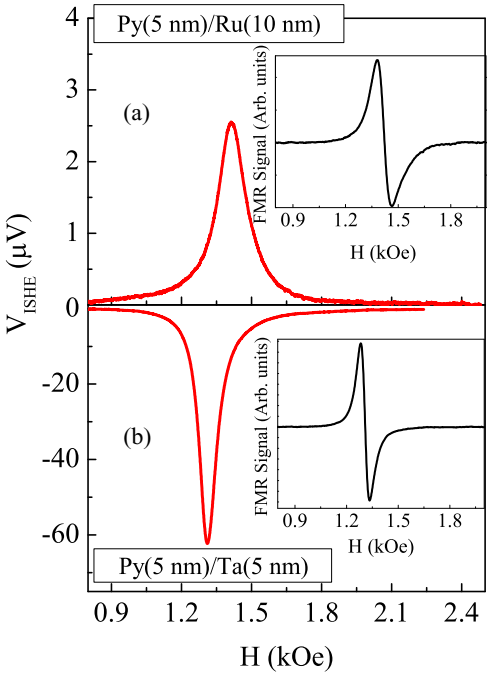

FIG. 2. (Color online) Typical voltage signal (V_{ISHE}) and FMR absorption spectra (inset) in two bilayers of Py in contact with different metals: (a) Ru; (b) Ta. The distance (L) between the electrical contacts is 2.2 and 2.3 mm, respectively.

typical FMR spectra and the corresponding V_{ISHE} measured on the bilayers Py(5 nm)/Ru(10 nm) and Py(5 nm)/Ta(5 nm). In the two samples the FMR absorption derivative has, as expected, near perfect odd symmetry with respect to the resonance field and the ISHE signal is close to symmetric which indicates that the contribution of anomalous Hall effect is small compared to the ISHE part [5]. In addition, one finds that the sign of the induced voltage is positive for Ru and negative for Ta.

The theory describing the spin injection from a FM layer fulfilling the resonance condition into an adjacent NM layer is well established [2,14,15] and numerous experimental results supporting these models can be found in the literature [5,6,16,17]. More precisely, a pure spin current appears as a consequence of an additional interfacial relaxation process, mediated by the conduction electrons of the normal metal, that contributes to relax the magnetization of the FM layer to the equilibrium configuration. This additional relaxation through the interface is added to the intrinsic volume relaxation of the FM and then an increment in the linewidth (ΔH) of the bilayer system is expected if compared with a single FM layer which is not in contact with a NM. Note that if the thickness of the FM layer is reduced, an increment of the linewidth is also expected because the interfacial relaxation process becomes more important when compared to volume processes, which are reduced by the decreasing thickness. The intrinsic linewidth is governed by the total Gilbert damping parameter α, and includes a thickness independent volume term (α_0) and an interfacial term that increases with decreasing thickness. The thickness dependence can be described by the following

expression [2]:

$$\alpha = \alpha_0 + \frac{\gamma}{4\pi M_s}\frac{\hbar}{t_{FM}} g^{\uparrow\downarrow}, \quad (1)$$

where $\gamma = g\mu_B/\hbar$ is the gyromagnetic ratio, g is the g factor, $\hbar$ is the reduced Planck constant, M_s is the saturation magnetization, and $g^{\uparrow\downarrow}$ is the effective spin mixing conductance. The quantity $g^{\uparrow\downarrow}$ is a property of the FM/NM interface and is phenomenologically interpreted as the net efficiency of the FM layer to transfer angular momentum across the FM/NM interface [18]. The parameter α_0 is the volume Gilbert damping parameter and is expected to be close to that of a single FM layer without any NM layer in contact.

In order to properly estimate the effective spin mixing conductance from the linewidth it is important to consider that ΔH is often enhanced by extrinsic contributions [19–21]. For example, the distribution of anisotropy axis (both in magnitude and orientation), inhomogeneities within the films, among other effects, can result in a wrong estimation of the parameter $g^{\uparrow\downarrow}$ if they are not properly considered. To separate the extrinsic contributions (which may be assumed to be independent of the excitation frequency) from the intrinsic relaxation, a linear frequency dependence of ΔH is often assumed and is phenomenologically described [22] by Eq. (2),

$$\Delta H = \Delta H_0 + \frac{2}{\sqrt{3}}\frac{\omega}{\gamma}\alpha. \quad (2)$$

In this equation the total peak-to-peak linewidth ΔH is the sum of the extrinsic contribution ΔH_0 and the intrinsic term proportional to the microwave excitation frequency $f = \omega/2\pi$.

We show in Fig. 3 the frequency dependence of ΔH for the set of samples (a) Py(t_{Py})/Ta(5 nm) and (b) Py(t_{Py})/Ru(10 nm) measured at X-, K-, and Q-band frequencies with the external field applied parallel to the film. We found that, within experimental error, the extrapolation to zero frequency yields $\Delta H_0 \approx 0$, indicating that the extrinsic contribution ΔH_0 is negligibly small in all cases. Note that we have neglected any extrinsic contribution coming from the two magnon scattering process based on the fact that similar linewidths were observed when the external field was applied parallel or perpendicular to the film plane. Also, the typical square root frequency dependence for this mechanism is not observable in the experimental data of Fig. 3. This figure shows an increment of the slope in both series of bilayers when the thickness of the Py layer is decreased. Analyzing these data by using Eq. (2) we can obtain the total Gilbert damping parameter for each sample and then, from the dependence of this parameter as a function of the inverse of the Py thickness [Eq. (1)], it is possible to separate the volume and interfacial relaxation terms. In Fig. 3(c) we plot α vs $1/t_{Py}$ and, by performing a linear fit, we estimated α_0 and the effective spin mixing conductance. We list in Table II the values of $g^{\uparrow\downarrow}$ and α_0 obtained for the two sets of samples. For this estimation we used a saturation magnetization $M_s = 770$ emu/cm^3. The procedure used to determine M_s and the surface anisotropy K_s is discussed in Sec. III B. As already mentioned, α_0 corresponds to the volume Gilbert damping parameter of the Py layer without the interfacial contribution to the relaxation. We obtained the same value for both bilayers, $\alpha_0 = 0.0083 \pm 0.0022$, that is

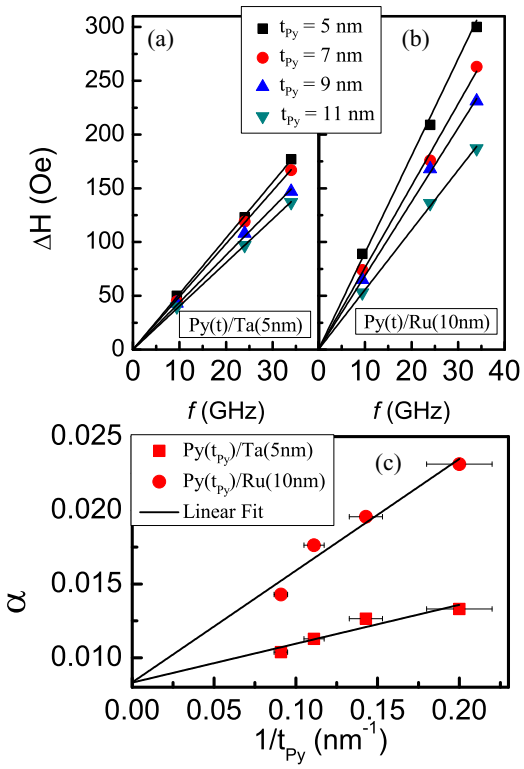

FIG. 3. (Color online) Dependence of the peak to peak linewidth of (a) Py(t_{Py})/Ta(5 nm) and (b) Py(t_{Py})/Ru(10 nm) series as a function of the microwave excitation frequency. (c) Total Gilbert damping parameter as a function of the inverse of the Py layer thickness for both sets of samples.

comparable to previous reports in Py which range between $\alpha_0 \sim 0.006$ [23] and $\alpha_0 \sim 0.013$ [24].

The value for the effective spin mixing conductance in the Py/Ru interface is about three times larger than $g^{\uparrow\downarrow}$ for Py/Ta. The spin current injected in the NM layer is proportional to $g^{\uparrow\downarrow}$ and can be estimated [14,16] from

$$J_s\hat{\mathbf{s}} = \frac{\hbar}{4\pi} g^{\uparrow\downarrow} \mathbf{m} \times \frac{d\mathbf{m}}{dt}, \quad (3)$$

where $\mathbf{m} = \frac{\mathbf{M}}{M_s}$ is the reduced magnetization. Thus, from the obtained values of $g^{\uparrow\downarrow}$, we can conclude that Ru mediates better than Ta the relaxation of the magnetization of the Py layer by creating a larger pure spin current.

In this work we have used a model similar to that developed in Ref. [16], by considering that the spin Hall voltage is originated by the injected spin current averaged over a time

TABLE II. Effective spin mixing conductance $g^{\uparrow\downarrow}$ and volume Gilbert damping parameter α_0 for the two series of samples Py(t_{Py})/Ta(5 nm) and Py(t_{Py})/Ru(10 nm) obtained from a linear fit of the data shown in Fig. 3(c).

Interface	$g^{\uparrow\downarrow}(10^{15}$ cm$^{-2})$	α_0
Py/Ta	1.3 ± 0.4	0.0083 ± 0.0012
Py/Ru	3.8 ± 0.7	0.0083 ± 0.0022

period. This results in a pure dc spin current propagating in the $\hat{x}$ direction (perpendicular to the interface) and polarized along the magnetization direction $\hat{s}$ [the reference system is sketched in Fig. 1(b)]. The dc pure spin current is converted into a charge current via the inverse spin Hall effect that deflects the electrons preferentially to one end of the sample. The edge of the sample where the charge accumulation takes place depends on the sign of the deflection of the carriers, given by the sign of the spin Hall angle, Θ_{SH},

$$\mathbf{J}_c = \Theta_{SH}\left(\frac{-2e}{\hbar}\right) J_s^x(\hat{x}\times\hat{s}), \tag{4}$$

where $\mathbf{J}_c$ is the charge current, J_s^x is the dc spin current that takes different values inside of the NM layer along the $\hat{x}$ direction, and e is the electron charge. The unit vectors $\hat{x}$ and $\hat{s}$ are the propagation and polarization directions of the spin current, respectively.

We mentioned that Py/Ru and Py/Ta samples have opposite signs of the measured V_{ISHE} signal (as can be seen in Fig. 2), from which we conclude that Ru and Ta have opposite spin Hall angle signs. This result was already pointed out in Ref. [25], and it is related to the fact that the sign of the spin Hall conductivity depends on the sign of the spin-orbit interaction, being positive for more than half-filled d orbitals (as happens in Ru, which has a $4d^7$ configuration, according to Hund's rules) and negative in the other case (Ta is a $5d^3$). The negative sign of the Ta spin Hall angle was experimentally observed in Ref. [6]. We have also observed that the ISHE voltage measured on these two kinds of bilayers (with the same Py thickness and similar electrodes separation) is always larger (about one order of magnitude) in the series with Ta, although the FMR linewidth and the effective spin mixing conductance were always larger in the Ru series.

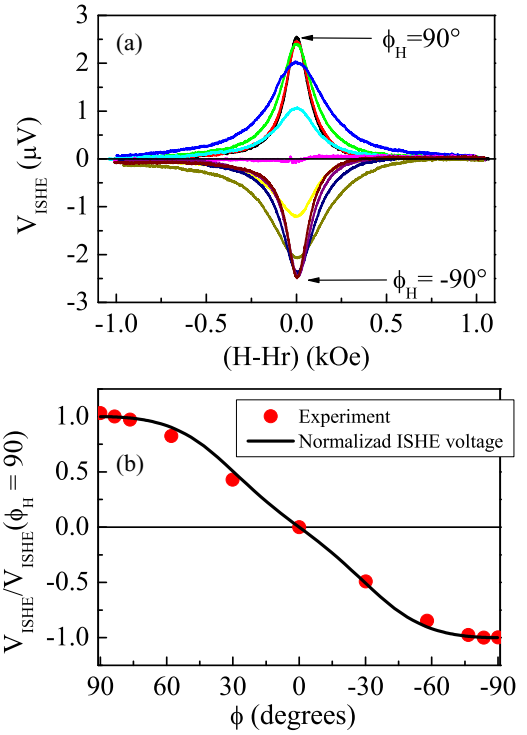

FIG. 4. (Color online) (a) ISHE voltage signal measured in an X-Band FMR experiment performed in the Py(5 nm)/Ru(10 nm) bilayer for different orientations of the magnetic field with respect to the film normal (ϕ_H). (b) Peak value of the symmetric contribution as a function of the angle of the equilibrium magnetization (ϕ) normalized by the V_{ISHE} acquired at $\phi_H = 90°$. The solid line corresponds to the values obtained from Eq. (9) using the FMR data. Explored angles are $\phi_H = \pm 90°, \pm 60°, \pm 40°, \pm 20°, \pm 10°$, and $0°$.

B. Angular variation of V_{ISHE} in the Ru series

As far as we know the inverse spin Hall voltage generated in a Py/Ru bilayer has not been yet reported, which led us to perform careful measurements to characterize the angular dependence of the V_{ISHE} signal on ϕ_H, the angle between the external magnetic field, **H**, and the film normal [see Fig. 1(b)].

We show in Fig. 4(a) the angular dependence of the voltage measured in the neighborhood of the FMR resonance field, in the sample Py(5 nm)/Ru(10 nm) at different angles, starting from $+90°$ and ending in $-90°$. We have centered the V_{ISHE} peak at the resonance field position to better appreciate the evolution of the spectra for different angles. We have fitted all measured spectra by an absorption (assumed of Lorentzian shape) and a dispersion curve (Lorentzian-like derivative) as suggested in Ref. [5]. With this procedure we could separate the ISHE signal from the contribution originating from the anomalous Hall effect in the FM layer, which are even and odd functions, respectively. From the fitting it is possible to extract the intensity of the symmetric component (V_{ISHE}), its field position (H_r), and linewidth (ΔH). As expected, these two last quantities coincide with the corresponding values measured in FMR experiments. The antisymmetric contribution in each of these spectra is very small as is readily observed in Fig. 4(a). Also, the intensity of the spectra at 90° is equal, within experimental error, but opposite in sign to that acquired at $-90°$, allowing us to discard any contributions coming from anisotropic magnetoresistance effects [5].

Figure 5 shows the angular dependence of the resonance field position and the linewidth of the bilayer Py(5 nm)/Ru(10 nm). A typical behavior for thin films is found, in which H_r is maximum when **H** is applied perpendicular to the film plane and ΔH peaks approximately where $\partial H_r/\partial\phi_H$ is maximum [26–28]. The Smit and Beljers formalism is generally used [22] to obtain the dispersion relation for the uniform mode of precession [Eq. (5)] and the equilibrium angle of the magnetization [Eq. (6)]. From the measurements of the resonance field with the applied field parallel and perpendicular to the film plane it is then possible to obtain the effective anisotropy field (H_{eff}) and the g value. Once the effective anisotropy field is calculated, from Eq. (6) it is possible to estimate the angle of equilibrium of the magnetization, ϕ. These quantities, H_{eff} and ϕ, are necessary for fitting the angular dependence of V_{ISHE}:

$$\left(\frac{\omega}{\gamma}\right)^2 = [H_r\cos(\phi_H-\phi) - H_{\mathrm{eff}}\cos^2(\phi)] \times [H_r\cos(\phi_H-\phi) - H_{\mathrm{eff}}\cos(2\phi)], \tag{5}$$

$$2H_r\sin(\phi_H-\phi) + H_{\mathrm{eff}}\sin(2\phi) = 0. \tag{6}$$

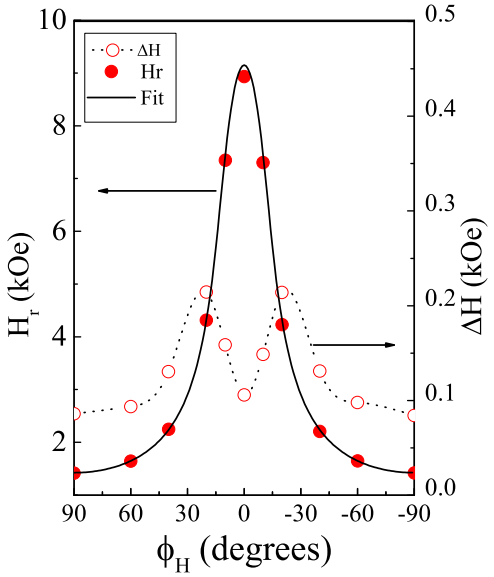

FIG. 5. (Color online) Angular variation of the resonance field (full symbols) and the linewidth (open symbols) in the bilayer Py(5 nm)/Ru(10 nm) obtained from X-Band FMR experiments. The solid line corresponds to the fitting using Eqs. (5) and (6), from which we obtained $H_{\text{eff}} = 5920$ Oe. The dotted line is a guide to the eye.

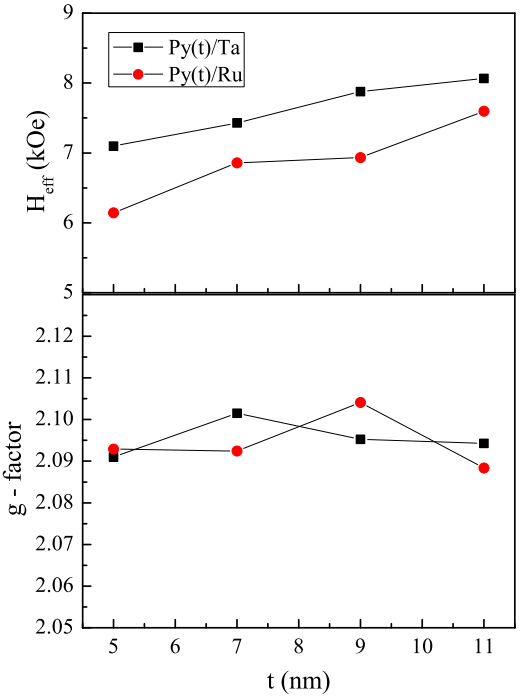

FIG. 6. (Color online) Thickness dependence of the effective anisotropy field (H_{eff}) and the g factor of the Py(t)/Ta and Py(t)/Ru series.

FMR experiments performed at parallel and perpendicular geometries for different Py thicknesses show a relatively constant g-factor value of $g = 2.095 \pm 0.009$ and a decreasing value of H_{eff} when the thickness of Py is reduced. The quantity H_{eff} is related to the shape anisotropy ($4\pi M_s$) of the sample, but in thin films the surface anisotropy must be also considered, especially for thicknesses in the nm range. The usual expression to consider these two anisotropies is given [29] by

$$H_{\text{eff}} = 4\pi M_s - \frac{4K_s}{M_s t_{\text{Py}}}, \tag{7}$$

where the last term is the surface anisotropy field written as a function of the surface anisotropy constant (K_s) and the Py thickness.

To estimate M_s, we used a reference thick film of approximately 313 nm, which is thick enough to discard surface effects. From the FMR data and Eq. (5) we deduced $M_s = 770$ emu/cm^3 and $g = 2.091$, which is coincident with the g value of Py obtained in the studied bilayers. Note that in very thin films a magnetically "dead" layer is often considered in order to account for the reduced magnetization of the surface layers which are in contact with the substrate or the nonmagnetic metal. In this situation the nominal thickness of the ferromagnetic layer should be corrected to an effective one. In the present work we used the nominal Py thickness and considered an uncertainty of 0.5 nm in the Py thicknesses to take into account the possible presence of a dead layer. Small departures from the proposed model could be due to this effect.

In Fig. 6 we show the dependence of the g factor and H_{eff} of the Py(t)/Ta and Py(t)/Ru series as a function of the inverse of the Py thickness. It is important to mention that values of H_{eff} were obtained in most cases using only the resonance field values parallel and perpendicular to the film plane. In Fig. 5 we fit the angular variation of the resonance field using all experimental points and although this procedure is expected to be more precise for the estimation of H_{eff} the differences between both methods are always smaller than a few percent.

By solving the Landau-Lifshitz-Gilbert equation of motion, and following the same reasoning of Ref. [16] it is possible to derive the angular dependence of the injected dc spin current at the resonance condition [i.e., when Eq. (5) is satisfied]

$$J_s^0(\phi) = \gamma \frac{\hbar}{4\pi} g^{\uparrow\downarrow} \left(\frac{h_{\text{RF}}}{\alpha}\right)^2 \times \left[\frac{[H_r \cos(\phi_H - \phi) - H_{\text{eff}} \cos(2\phi)]}{[2H_r \cos(\phi_H - \phi) - H_{\text{eff}}(3\cos^2\phi - 1)]^2}\right], \tag{8}$$

where h_{RF} is the amplitude of the microwave magnetic field inside of the resonant cavity. This expression is totally equivalent to Eq. (12) of Ref. [16], but has been rearranged to emphasize the dependence on the effective anisotropy field and the relative orientation between the magnetization and the external field.

The spin current shown in Eq. (8) corresponds to the current at the interface of the FM/NM bilayer that propagates diffusively inside the NM layer. Using the coordinate system shown in Fig. 1(b) and from Eq. (4) one can figure out that the pure spin current propagates in x direction and is polarized along the magnetization direction. As $V_{\text{ISHE}} \propto J_s^0(\phi)\sin(\phi)$, it is convenient to define a normalized spin Hall effect voltage

as

$$V_N = \frac{J_s^0(\phi)}{J_s^0(\phi = 90^\circ)} \sin(\phi) = \frac{[H_r \cos(\phi_H - \phi) - H_{\text{eff}} \cos(2\phi)]}{[2H_r \cos(\phi_H - \phi) - H_{\text{eff}}(3\cos^2\phi - 1)]^2} \times \frac{[2H_{||} + H_{\text{eff}}]^2}{H_{||} + H_{\text{eff}}} \sin(\phi), \quad (9)$$

where we defined $H_{||}$ as the resonance field measured at $\phi = \phi_H = 90^\circ$. The normalized experimental data of Fig. 4(b) has been superimposed with the curve obtained from Eq. (9), which depends exclusively on parameters obtained from the FMR spectra. A very close agreement was found, supporting the proposed model.

C. Microwave power dependence

We also studied the microwave power (P) dependence of the ISHE voltage in the sample Py(5 nm)/Ru(10 nm). All measurements were performed with the external field parallel to the plane of the sample along the y direction. We show in Fig. 7 the obtained linear behavior of the maximum of the measured voltage as a function of P. As explained in the literature [16] this is a consequence of the dependence of Eq. (8) with h_{RF}^2. To understand the linear dependence of V_{ISHE} as a function of P we can inspect the time averaged y component of Eq. (3), $J_s^0 \propto \int_0^{\frac{2\pi}{\omega}} [m_x \frac{dm_z}{dt} - m_z \frac{dm_x}{dt}]dt$. As we are in the linear response regime ($\mathbf{m} = \underline{\chi}\mathbf{h}_{\text{RF}}$) each transversal component $m_{i=x,z}$ contributes with a h_{RF} factor, making $J_s^0 \propto h_{\text{RF}}^2$ and hence $V_{\text{ISHE}} \propto h_{\text{RF}}^2$. As P is proportional to h_{RF}^2 [30] we obtain the linear behavior of the maximum of the measured voltage as a function of the microwave power, as shown in Fig. 7.

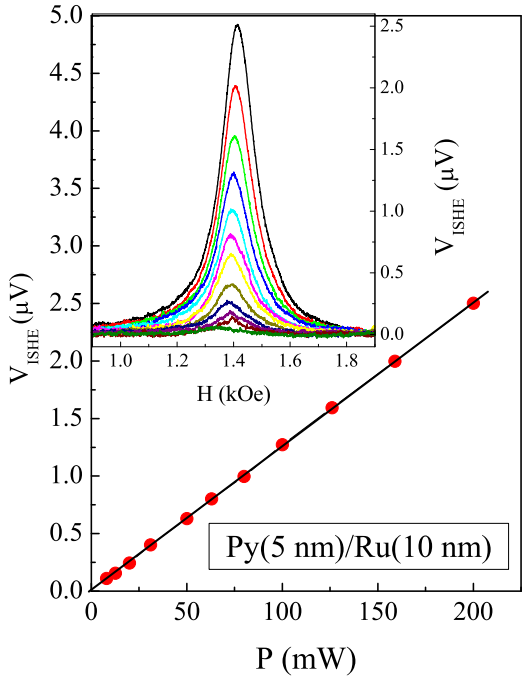

FIG. 7. (Color online) Power dependence of the maximum inverse spin Hall voltage measured at $H = H_r$. In the inset we show the Lorentzian shape of V_{ISHE} curves in the neighborhood of H_r. Data correspond to the bilayer Py(5 nm)/Ru(10 nm) varying P from 4 mW to 200 mW.

D. Estimation of the transport parameters in the Py/Ta series

To estimate the transport parameters involved in the ISHE effect, we have studied two different series of Py/Ta bilayers. The first set, Py(t_{Py})/Ta(5 nm), has variable Py thickness with $t_{\text{Py}} = 5$, 7, 9, and 11 nm and a fixed thickness of 5 nm for the Ta layer. The second series, Py(10 nm)/Ta(t_{Ta}), has the same Py thickness in all samples and the Ta layer thickness takes the values $t_{\text{Ta}} = 2$, 5, 8, and 11 nm. In all cases we have acquired the voltage signal by applying the magnetic field in the plane of the sample with a microwave power $P = 200$ mW. To perform the analysis we have extracted the V_{ISHE} symmetric contribution of the signal, as already explained.

The dc spin current injected by the spin pumping phenomena diffusively propagates in the NM layer and, via the inverse spin Hall effect, it is converted into a charge current. Because we work in an open circuit condition, this charge current creates an electric field that cancels its propagation. The theory and expression for the resulting voltage, see Eq. (10), associated to this electric field is well established and can be found in several articles [9,16],

$$V_{\text{ISHE}} = L \left(\frac{2e}{\hbar}\right) \frac{\Theta_{SH}\lambda_{SD} \tanh(t_{\text{Ta}}/2\lambda_{SD})}{t_{\text{Py}}\sigma_{\text{Py}} + t_{\text{Ta}}\sigma_{\text{Ta}}} J_s^0. \quad (10)$$

In this equation L is the separation between the electrodes where the voltage is measured, λ_{SD} is the spin diffusion length, and σ_{Py} and σ_{Ta} are the electrical conductivities of Py and Ta, respectively.

All FMR effects are contained in J_s^0 that takes the form of Eq. (11) when the external field is applied parallel to the film plane ($\phi_H = \phi = 90^\circ$)

$$J_s^0 = \gamma \frac{\hbar}{4\pi} g^{\uparrow\downarrow} \left(\frac{h_{\text{RF}}}{\alpha}\right)^2 \frac{H_{||} + H_{\text{eff}}}{[2H_{||} + H_{\text{eff}}]^2}. \quad (11)$$

Combining Eq. (10) with Eq. (11) we can define the quantity $\overline{\rho}$

$$\overline{\rho} = \frac{V_{\text{ISHE}}}{L} \left(\frac{2\pi}{e}\right) \frac{\alpha^2}{\gamma g^{\uparrow\downarrow}} \left[\frac{[2H_{||} + H_{\text{eff}}]^2}{H_{||} + H_{\text{eff}}}\right] = h_{\text{RF}}^2 \frac{\Theta_{SH}\lambda_{SD} \tanh(t_{\text{Ta}}/2\lambda_{SD})}{t_{\text{Py}}\sigma_{\text{Py}} + t_{\text{Ta}}\sigma_{\text{Ta}}} \quad (12)$$

that, apart from a factor h_{RF}^2, has units of resistivity (Ω nm). In Fig. 8 we show the $\overline{\rho}$ curves obtained as a function of magnetic field for each series. As expected from Eq. (12), $\overline{\rho}$ decreases when t_{Py} increases and has a more complex behavior as a function of t_{Ta}. This suggests that the marked different behavior of $\overline{\rho}$ with t_{Py} and t_{Ta} may be used to extract separately the values of λ_{SD} and Θ_{SH}. We obtained the maximum of the symmetric contribution in each of the curves, normalized this value in order to calculate $\overline{\rho}$, and plotted this variable as a function of t_{Py} and t_{Ta}, in Figs. 9(a) and 9(b), respectively. In Fig. 9(a) we can observe that the experimental $\overline{\rho}$ as a function of t_{Py} follows approximately the hyperbolic functional dependence

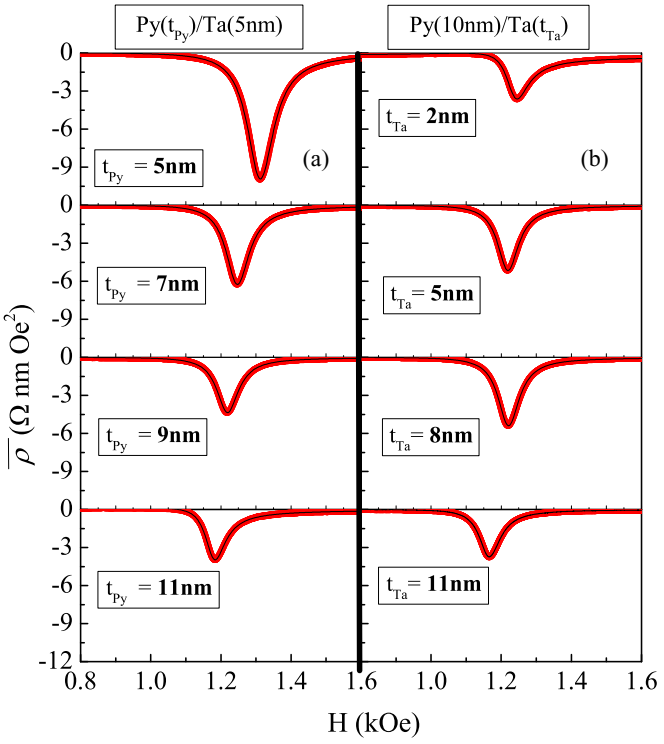

FIG. 8. (Color online) $\overline{\rho}$ signal as a function of magnetic field for (a) Py(t_{Py})/Ta(5 nm) and (b) Py(10 nm)/Ta(t_{Ta}) series.

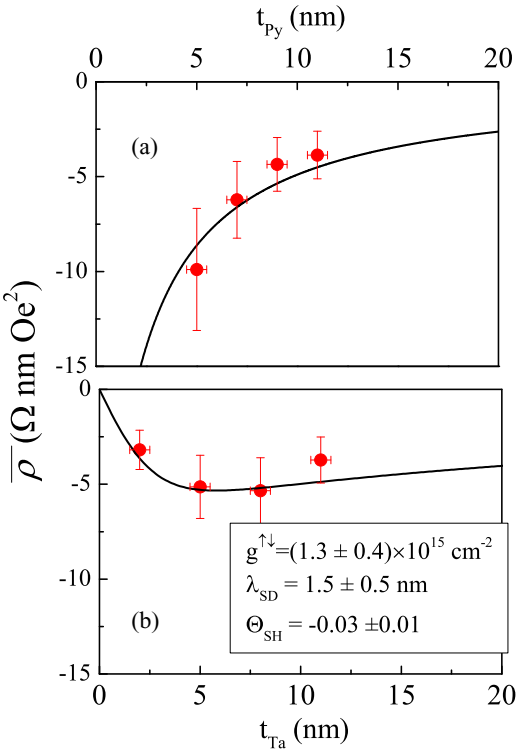

FIG. 9. (Color online) Dependence of $\overline{\rho}$ as function of the thickness of (a) Py layer and (b) Ta layer. The continuous lines are the fits obtained with Eq. (12) and the parameters indicated in the figure.

of Eq. (12), $\overline{\rho}(t_{Py}) = K/(t_{Py}\sigma_{Py} + t_{Ta}\sigma_{Ta})$. Using the bulk conductivities of Ta and Py [10,31], $\sigma_{Ta} = 0.0005\ \Omega^{-1}\text{nm}^{-1}$and $\sigma_{Py} = 0.0022\ \Omega^{-1}\text{nm}^{-1}$, and fitting the experimental data we have obtained $K = 0.091(7)$ (Oe^2 nm).

The constant K can then be used to fit the experimental values of $\overline{\rho}$ as a function of t_{Ta} for a fixed value of t_{Py} using

$$\overline{\rho}(t_{Ta}) = \frac{1}{t_{Py}\sigma_{Py} + t_{Ta}\sigma_{Ta}} \frac{K}{\tanh\frac{5}{2\lambda_{SD}}} \tanh\frac{t_{Ta}}{2\lambda_{SD}}. \qquad (13)$$

The best fit of the experimental data is shown in Fig. 9(b) and was obtained for $\lambda_{SD} = 1.5 \pm 0.5$ nm.

It is important to note here that this procedure allowed us to experimentally determine the spin diffusion length in Ta without knowing the spin Hall angle Θ_{SH} or the microwave field amplitude h_{RF}.

With this estimation of λ_{SD} and knowing the value of h_{RF}, it is possible to calculate Θ_{SH}. The TE_{102} resonant cavity used in our experiment has a quality factor $Q \sim 2400$ (defined as $Q = \omega/\Delta\omega$) that was not significantly changed when the sample was placed inside. With this value of Q and following Ref. [32] we estimated $h_{RF} \sim 1.5(3)$ Oe, obtaining $\Theta_{SH} \sim -0.03 \pm 0.01$. It is worth mentioning that the experimental determination of h_{RF} is not straightforward and usually comes with a large associated error. As a consequence, the spin Hall angle is also expected to be affected by a large uncertainty, and was estimated to be around 50% in our case.

We also note that our fittings of the experimental data were made using the bulk electrical conductivities of Ta and Py. It is well known that the conductivity depends on film thickness, and the correction becomes important when the thickness is reduced to 1 nm or less [33]. If we consider this correction only a minor improvement is obtained in our data. However, there are reports in the literature in which an experimental thickness dependence of the conductivity of Ta [6] and Py [15] is observed well above 1 nm. If we take into account these values a slightly better fit of the experimental data can be obtained but the spin diffusion length is almost unaffected.

IV. CONCLUSIONS

In summary, we have studied two bilayer systems, Py/Ru and Py/Ta, as a function of the permalloy thickness t_{Py}. In both systems we estimated the effective spin mixing conductance by analyzing the dependence of the FMR linewidth as a function of t_{Py}. We obtained a larger value of $g^{\uparrow\downarrow}$ in the Py/Ru system indicating that Ru mediates better the relaxation of the magnetization of the Py layer during the resonance, creating a larger pure spin current. In the same analysis, extrapolating the tendency of the Gilbert damping parameter as a function of the inverse of the film thickness, we have found $\alpha_0 = 0.0083 \pm 0.0022$ for the polycrystalline Py layer in both systems.

Because the ability of Ru to convert a pure spin current into a charge current has not been yet reported, we explored the angular and microwave power dependence of the inverse spin Hall voltage in the Py/Ru system obtaining an excellent agreement with the predictions of the inverse spin Hall effect theory. On the other hand, we estimated the spin diffusion length and the spin Hall angle of Ta by analyzing the dependence of the inverse spin Hall voltage in this system as a function of both Py and Ta layer thicknesses obtaining $\lambda_{SD} =$

1.5 ± 0.5 nm and $\Theta_{SH} = -0.03 \pm 0.01$ in agreement with recently published results [6]. We have also experimentally verified that Ru and Ta have opposite spin Hall angle signs.

Comparing both systems we have found that Ru produces a larger spin current but, because of its higher conductivity and probably a smaller spin Hall angle, it produces a weaker inverse spin Hall voltage. On the contrary, despite its relatively small $g^{\uparrow\downarrow}$ value, Ta generates a larger V_{ISHE} because of its higher resistivity and a larger spin Hall angle. The latter result makes Ta a good candidate to be used as a spin current detector without affecting considerably the Py magnetization relaxation.

ACKNOWLEDGMENTS

This work was supported by Conicet (Grant No. PIP 112-201101-00482), ANPCyT (Grant No. PICT-2010-0773), and U.N. Cuyo (Grant No. 06/C352), all from Argentina. Investment funds for advanced electron-paramagnetic resonance instrumentation from the Flemish Hercules foundation in Project No. AUHA013 and support from the MINCyT–FWO international cooperation project (No. FW/11/04) are kindly acknowledged. We would also like to acknowledge the very fruitful discussions with Dr. Juan Carlos Rojas Sánchez.

[1] F. Mott, Proc. R. Soc. A **153**, 699 (1936); M. Johnson and R. H. Silsbee, Phys. Rev. Lett. **55**, 1790 (1985); T. Valet and A. Fert, Phys. Rev. B **48**, 7099 (1993).
[2] Y. Tserkovnyak, A. Brataas, and G. E. W. Bauer, Phys. Rev. Lett. **88**, 117601 (2002).
[3] E. Saitoh, M. Ueda, H. Miyajima, and G. Tatara, Appl. Phys. Lett. **88**, 182509 (2006).
[4] K. Uchida, S. Takahashi, K. Harii, J. Ieda, W. Koshibae, K. Ando, S. Maekawa, and E. Saitoh, Nature (London) **455**, 778 (2008); Y. Kajiwara, K. Harii, S. Takahashi, J. Ohe, K. Uchida, M. Mizuguchi, H. Umezawa, H. Kawai, K. Ando, K. Takanashi, S. Maekawa, and E. Saitoh, *ibid.* **464**, 262 (2010).
[5] O. Mosendz, J. E. Pearson, F. Y. Fradin, G. E. W. Bauer, S. D. Bader, and A. Hoffmann, Phys. Rev. Lett. **104**, 046601 (2010).
[6] C. Hahn, G. de Loubens, O. Klein, M. Viret, V. V. Naletov, and J. Ben Youssef, Phys. Rev. B **87**, 174417 (2013).
[7] C. T. Boone, H. T. Nembach, J. M. Shaw, and T. J. Silva, J. Appl. Phys. **113**, 153906 (2013).
[8] H. Kurt, R. Loloee, K. Eid, W. P. Pratt, Jr., and J. Bass, Appl. Phys. Lett. **81**, 4787 (2002).
[9] J. C. Rojas-Sánchez, N. Reyren, P. Laczkowski, W. Savero, J. P. Attané, C. Deranlot, M. Jamet, J. M. George, L. Vila, and H. Jaffrès, Phys. Rev. Lett. **112**, 106602 (2014).
[10] J. Lin, J. J. Moore, W. D. Sproul, S. L. Lee, and J. Wang, IEEE Trans. Plasma Sci. **38**, 3071 (2010).
[11] R. Hoogeveen, M. Moske, H. Geisler, and K. Samwer, Thin Solid Films **275**, 203 (1996).
[12] L. A. Clevenger, A. Mutscheller, J. M. E. Harper, C. Cabral, Jr., and K. Barmak, J. Appl. Phys. **72**, 4918 (1992).
[13] D. W. Face and D. E. Prober, J. Vac. Sci. Technol. A **5**, 3408 (1987).
[14] A. Brataas, Y. Tserkovnyak, G. E. W. Bauer, and B. I. Halperin, Phys. Rev. B **66**, 060404(R) (2002).
[15] H. J. Jiao and G. E. W. Bauer, Phys. Rev. Lett. **110**, 217602 (2013).
[16] K. Ando, S. Takahashi, J. Ieda, Y. Kajiwara *et al.*, J. Appl. Phys. **109**, 103913 (2011).
[17] H. Y. Inoue, K. Harii, K. Ando, K. Sasage, and E. Saitoh, J. Appl. Phys. **102**, 083915 (2007).
[18] O. Mosendz, V. Vlaminck, J. E. Pearson, F. Y. Fradin, G. E. W. Bauer, S. D. Bader, and A. Hoffmann, Phys. Rev. B **82**, 214403 (2010).
[19] N. Álvarez, G. Alejandro, J. Gómez, E. Goovaerts, and A. Butera, J. Phys. D: Appl. Phys. **46**, 505001 (2013).
[20] A. Butera, N. Álvarez, G. Jorge, M. M. Ruiz, J. L. Mietta, and R. M. Negri, Phys. Rev. B **86**, 144424 (2012).
[21] A. Butera, Eur. Phys. J. B **52**, 297 (2006).
[22] J. Gómez and A. Butera, Physica B **354**, 145 (2004).
[23] K. Kobayashi, N. Inaba, N. Fujita, Y. Sudo, T. Tanaka, M. Ohtake, M. Futamoto, and F. Kirino, IEEE Trans. Magn. **45**, 2541 (2009).
[24] B. K. Kuanr, R. E. Camley, and Z. Celinski, J. Magn. Magn. Mater. **286**, 276 (2005).
[25] A. Hoffmann, IEEE Trans. Magn. **49**, 5172 (2013).
[26] A. Butera, J. N. Zhou, and J. A. Barnard, Phys. Rev. B **60**, 12270 (1999).
[27] E. Burgos, E. Sallica Leva, J. Gómez, F. Martínez Tabares, M. Vásquez Mansilla, and A. Butera, Phys. Rev. B **83**, 174417 (2011).
[28] A. Butera, J. Gómez, J. L. Weston, and J. A. Barnard, J. Appl. Phys. **98**, 033901 (2005).
[29] M. Getzlaff, *Fundamentals of Magnetism* (Springer, New York, 2008), p. 112.
[30] G. Pake, *Paramagnetic Resonance, An Introductory Monograph* (W. A. Benjamin, New York, 1962), p. 41.
[31] A. C. Reilly *et al.*, J. Magn. Magn. Mater. **195**, L269 (1999).
[32] C. P. Poole, Jr., *Electron Spin Resonance: A Comprehensive Treatise on Experimental Techniques*, 2nd ed. (John Wiley and Sons, Inc., New York, 1983), p. 166.
[33] J. Milano and A. M. Llois, J. Appl. Phys. **102**, 013705 (2007).